CHARACTERIZATION AND UPGRADING OF ABU SHAAR MANGANESE ORES USING DRY HIGH-INTENSITY MAGNETIC SEPARATION

Mostafa El-Wekil[1], Khaled E. Yassin[2], Sayed A. Abouellaban[1], Ayman A. Hagrass[3*]

[1]Egyptian Mineral Resources Authority (EMRA), Abbasia, Cairo, Egypt.
[2]Central Metallurgical Research & Development Institute (CMRDI), Helwan, Cairo, Egypt.
[3]Mining and Metallurgy Department, Tabbin Institute for Metallurgical Studies (TIMS), Helwan, Cairo, Egypt.
***Corresponding author:** A. A. Hagrass (aahagrass@gmail.com)

ABSTRACT
Currently, the high-grade resources of manganese ores are decreased, and the high-grade ores are gradually depleted. Hence, the upgrading of low-grade manganese ores in an efficient way has become essential in terms of sustainable innovation for industry development. In this study, high-grade manganese could be effectively recovered from oolitic low-grade manganese ore, which is located in the Abu Shaar area, northwest of Hurghada. Characterization study of the head sample was carried out by X-ray diffraction (XRD), X-ray fluorescence (XRF), scanning electron microscopy (SEM), energy dispersive x-ray analysis (EDX) and petrography microscopic investigation. The effect of the attrition scrubbing process and dry magnetic separation technique on the upgrading of low-grade manganese ore was investigated. The attrition scrubbing process combined with the dry magnetic separation technique showed a great role in promoting MnO content, which increased from 33.72 to 44.12%, with a recovery efficiency of 77.22% in -500+250um size fraction. Also, the grade of MnO increased from 35.19 to 40.23%, with a recovery efficiency of 84.93% in -250+75um size fraction.

Keywords
Manganese; magnetic separation; attrition scrubbing; upgrading; Abu Shear

1. INTRODUCTION
Manganese ores are very important resources for the metallurgical and non-metallurgical industries such as ferrous metallurgy, non-ferrous metallurgy, industrial food applications, the chemical industries, dry battery cells, painting materials, agriculture and preparation of dietary additives, fertilizer additives and alloy agent in iron and steel industry [1-4]. Owing to the increasing demand for manganese ores and the gradual depletion of high-grade deposits, attention has turned to low-grade manganese ores, which contain various impurities [5-6].

The beneficiation of low-grade manganese ores economically and effectively is increasingly important [7]. The manganese ores in nature are mainly pyrolusite (MnO_2), cryptomelane (KMn_5O_{16}), psilomelane ($BaMn_9O_{16}(OH)_4$), manganite ($Mn_2O_3H_2O$) and rhodochrosite ($MnCO_3$) [8-9]. Beneficiation methods of manganese ore include physical methods (ore washing, magnetic separation, gravity separation), physio-chemical

(flotation), pyrometallurgy (roasting) and chemical (leaching) [10-17]. Low-grade manganese ores have many beneficiation problems due to their complex mineral association and their variable physical characteristics. Some of these problems cannot be overcome satisfactorily [18]. Calcination of manganese carbonate ores releases carbon dioxide, which causes environmental problems and high energy consumption, which is obviously unsuitable for the current environmental protection requirements [19].

Oolitic manganese ores, which contain chemically associated calcium, can be used as a fluxing agent during pyrometallurgical processing. These ores mainly require additional energy during pyrometallurgical processing due to the endothermic decomposition of carbonates, so these ores are more suitable for producing manganese compounds, considering their physical and chemical properties [20]. Wu et al. investigated reduction roasting to upgrade low-grade carbonate ores. They reported that the formation of complex manganese and iron magnetic phases ($MnFe_2O_4$, etc.) is useful for upgrading these types of ores. The results showed that the ore with an average initial grade of 10.39% manganese could be concentrated by high-intensity magnetic separation to obtain a product at a grade of 22.75% manganese at a recovery of 89.88%.[10].

S. Yuan et al. studied the beneficiation of low-grade ferromanganese ore via fluidization magnetization roasting and magnetic separation methods. The results illustrated that under the optimized conditions, high-quality products of manganese concentrate with a manganese grade of 53.30% at a manganese recovery of 90.41% were obtained. The fluidization magnetization roasting technology can make the pyrolusite and braunite transform into manganosite [21].

L. Gao et al. studied the beneficiation of high-alumina ferruginous manganese ores by the carbothermal roasting reduction process followed by the dry magnetic separation method. The grade and recovery of manganese were 54.35% and 90.05% respectively [22]. W. Ur Rehman et al. evaluated manganese ore beneficiation by using a high-intensity magnetic separator. Manganese content increased from 27% in the original sample to 45% in the concentrated sample, with a 23% recovery at 8500 Gauss [23]. G. Chen et al. applied microwave heating to the leaching of manganese from pyrolusite using pyrite as a reductant. The results showed that the manganese extraction rate reached 93.03% under the optimum parameters, while by conventional heating under the same conditions, the manganese extraction rate was only 75.84% [8].

The present work’s objective is upgrading Abu Shaar manganese ore to be suitable for the steel industry and different industrial applications. This purpose was achieved by dry magnetic separation technology after attrition scrubbing. Due to low energy consumption and the current environmental protection requirements, magnetic separation without calcination was selected in this study. The effects of particle sizes and magnetic intensity on the upgrading of manganese ore were investigated.

2. GEOLOGICAL SETTING OF THE STUDY AREA

Abu Shaar manganese mine is located in the southwestern part of the Esh el Mallahah ranges mountains, northwest of Hurghada, between Latitude 27º 22' 40" - 27º 21' 40" N, and longitude 33º 33' 00" - 33º 34' 30" E, Fig. (1). The area is characterized by a group of small and medium-sized hills of Marley limestone and topped by international limestone,

which forms most of the heads of these hills. The region is intersected by a network of wadis to the east direction, draining into Wadi Abu Shaar and eventually pouring to the east into the Red Sea.

The study includes surveying of the region, where approximately 3,000 cadastral points have already been monitored, including longitude, latitude, and height coordinates x, z, y, using modern programs Arc Globe, Arc Scene, Arc Map, through which the area can be shown in 3D, also by measuring different sectors and collecting many samples, Fig. (2). There are many exposers in the area that indicate the presence of ore close to the surface that increasing to the south as it goes to the southwestern plateau overlooking Wadi Beli (southwest of the mine site). The ore is found in the layers close to the surface in the southwestern mine plateau, which is topped by limestone intrusions 6 to 12 meters thick whenever heading south.

The stratigraphic sequence of the section can be described from top to bottom as follows:

1. Dolomitic limestone is relatively hard, has an average thickness of about 6 meters, and represents approximately 50% of the hill's areas.
2. Limestone: medium hardness changes horizontally to Marley limestone with an average thickness of approximately 6 meters and covers almost all hills.
3. Marl: In some parts, it has an average thickness of approximately 0.5 meters, representing approximately 20% of the slice areas.
4. Manganese ore: It has an average thickness of approximately 0.5-0.80 meters and represents approximately 70% of the hill areas.

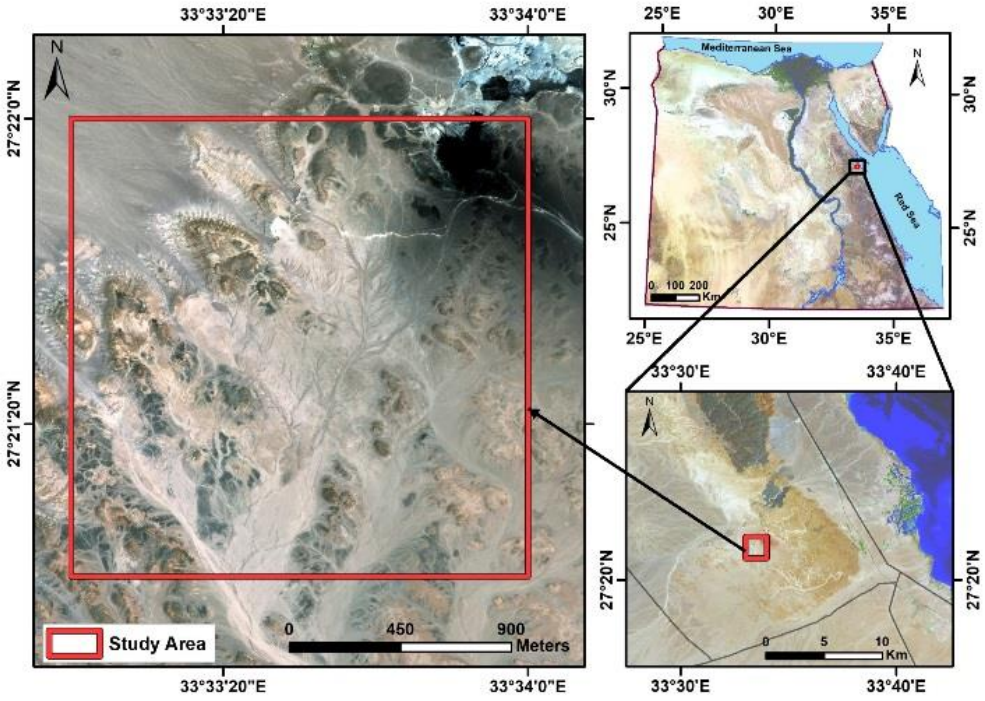

Fig. (1): Location map of the study area.

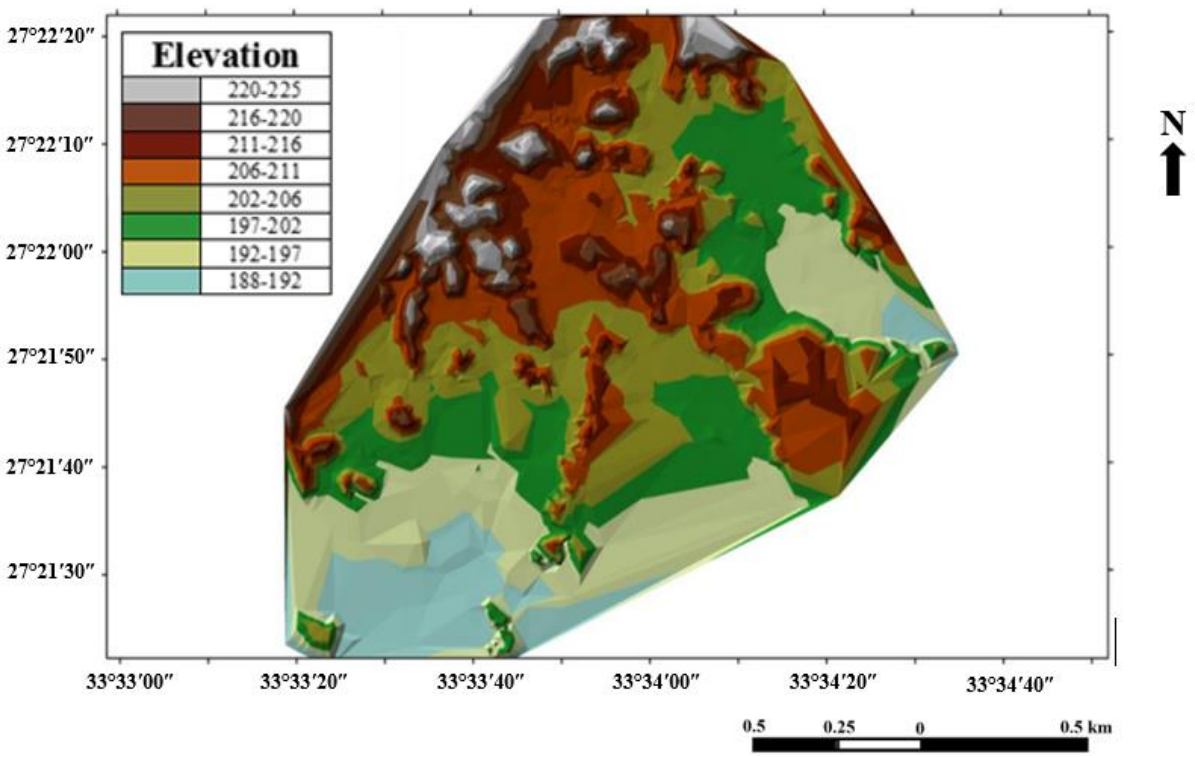

Fig. (2): Elevation map of the study area.

3. MATERIALS AND METHODS

About two hundred kilograms of a technologically representative low-grade manganese ore sample was collected from the Abu Shaar mine. The manganese sample was thoroughly directed to mixing and splitting preparation. A complete chemical analysis of the samples was carried out using the X-ray fluorescence (XRF) technique to determine various oxides such as MnO, SiO_2, Fe_2O_3, and CaO. X-ray diffraction (XRD) analysis was conducted by XRD diffractometer (model "Bruker axs, D8 Advance) to determine the phase composition of the minerals. The morphology and elemental compositions of the head sample were analyzed by scanning electron microscopy (SEM) and energy dispersive x-ray analysis (EDX), respectively. Petrography microscopic was investigated using reflected and transmitted light microscopy to determine the types of manganese ore and accompanied minerals and their textural relationships in the sample.

Comminution and sizing were applied to provide appropriate particle size for processing. The bulk manganese sample was directed to crushing using (5″X6″) Denver jaw crusher and (6 "x10") Denver roller crusher to produce a -5 mm crushed product. The product was ground to -500µm by using a laboratory rod and ball mills. Crushed and milled samples were classified into different size fractions using ASTM standard sieve analysis using a laboratory Retsch™ vibratory sieve shaker. The milled product was then directed to aggressive attrition scrubbing using a Denver (D-12) attrition scrubber machine at 65% solids, 1800 rpm motor speed, and 30 min. attrition time. The milled sample before and after attrition scrubbing was directed to the laboratory Carpco dry high intensity magnetic separator (Lift-type induced roll, Model MLH-13-111-5).

4. RESULTS AND DISCUSSION

4.1. Head sample characterization

Complete chemical analysis of the original sample using XRF analysis indicated that the sample contains 30.58% MnO and 29.5% loss of ignition, 15.56% CaO, 8.28% MgO, 5.80% SiO_2 and some minor amounts of P_2O_5, Al_2O_3, Na_2O, and Fe_2O_3 as shown in Table (1). The results showed that low grades in accordance with market standards for the manufacturing of many industries. The X-ray diffraction pattern of the manganese sample shows the distinguished d-spacing peaks which are related to pyrolusite (MnO_2), dolomite ($CaMg(CO_3)_2$), quartz (SiO_2), gypsum ($CaSO_4(H_2O)_2$), wustite minerals (FeO), Fig. (3). The morphology and elemental compositions of the head sample were analyzed by scanning electron microscopy (SEM) and energy dispersive x-ray analysis (EDX) respectively. The scanning electron microscope picture of the head sample indicates the major sample components are manganese and calcium carbonate. Manganese and calcium are the two major elements identified by EDX analysis, Fig. (4).

Petrography microscopic investigated the different types of accompanied minerals in the sample. These minerals are oolitic manganese ore (mainly pyrolusite) cemented by carbonate material (mainly dolomite) and associated with iron oxides, minor amounts of quartz, feldspar, traces of clay minerals and gypsum, Fig. (5). The mineralogical study showed that the upgrading of the ore by magnetic separation technique is possible because pyrolusite has significant difference in its magnetic susceptibility, where pyrolusite is a paramagnetic mineral while other accompanied impurities are diamagnetic minerals.

Table (1): Complete chemical analysis of the manganese head sample.

Oxide	Na_2O	MgO	Al_2O_3	SiO_2	P_2O_5	K_2O	CaO	MnO	Fe_2O_3	L.O.I.
%	0.43	8.28	2.10	5.80	0.43	1.02	15.56	30.58	1.03	29.5

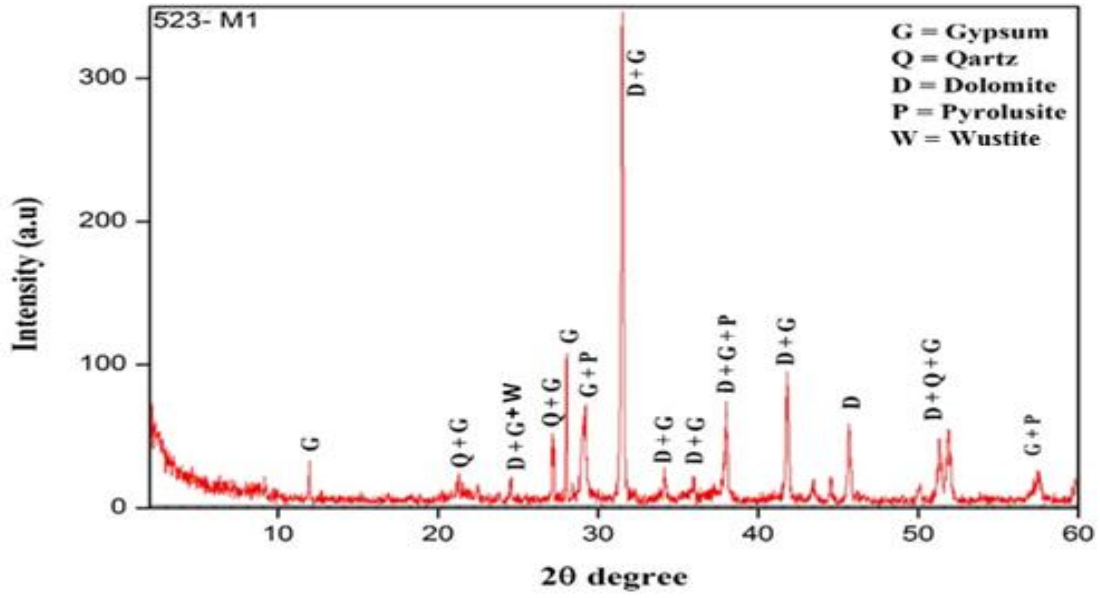

Fig. (3): XRD patterns of the manganese sample.

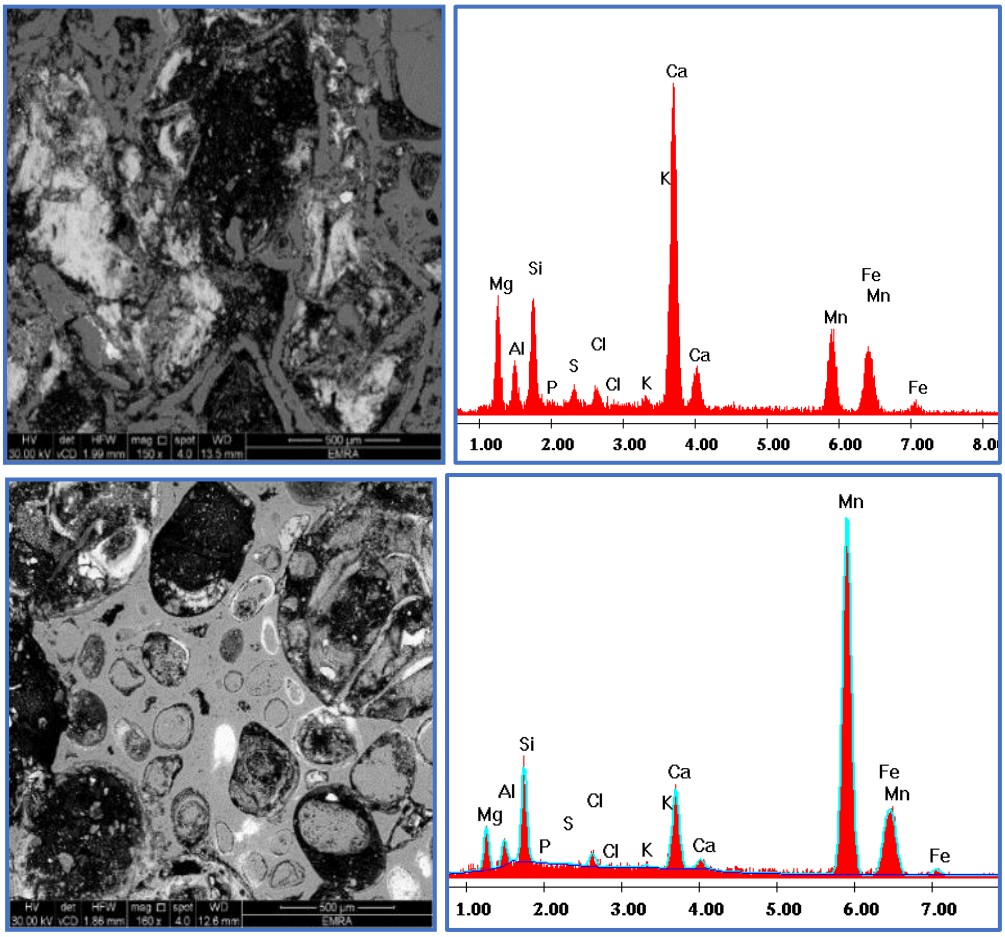

Fig. (4): Scanning electron microscope micrograph and EDX pattern of the manganese head sample.

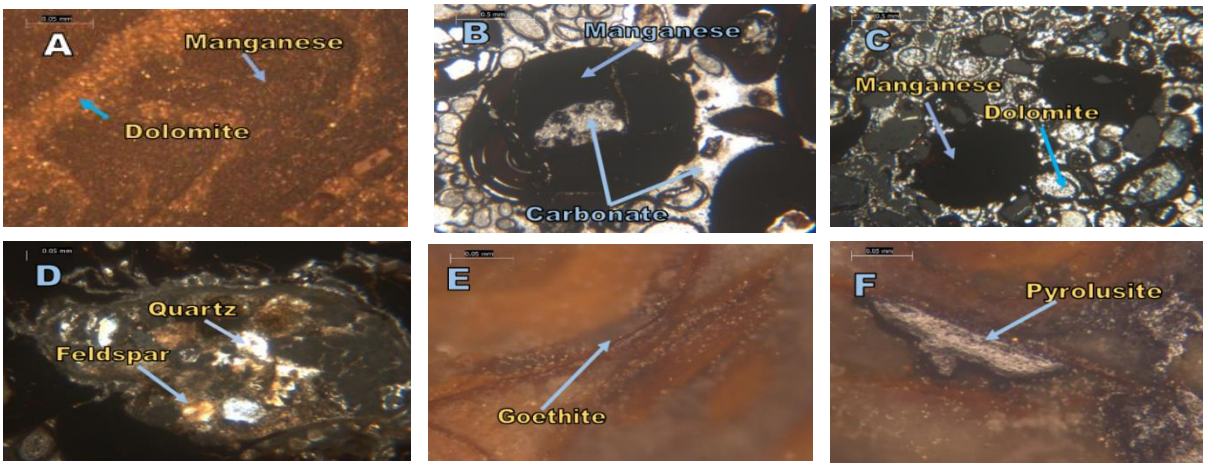

Fig. (5): Manganese micro crystalline under crossed nicol, (B) and (C) Plain polarized light image showing manganese oolites found as alternate concentric layers with carbonates in the form of oolits , (D) Quartz and feldspar in matrix, (E) Iron oxide (goethite) in the carbonate matrix, and (F) Pyrolusite as alternate concentric layers with carbonates.

4.2. Sieve and chemical analyses of crushed manganese size fractions

The head sample of the manganese sample was primarily crushed -5mm using the laboratory scale, namely the "Denver" jaw crusher. The dry particle size distribution of the crushed manganese sample showed that the D_{50} value was 0.62mm, while the D_{80} value was above 2.3mm, Fig. (6).

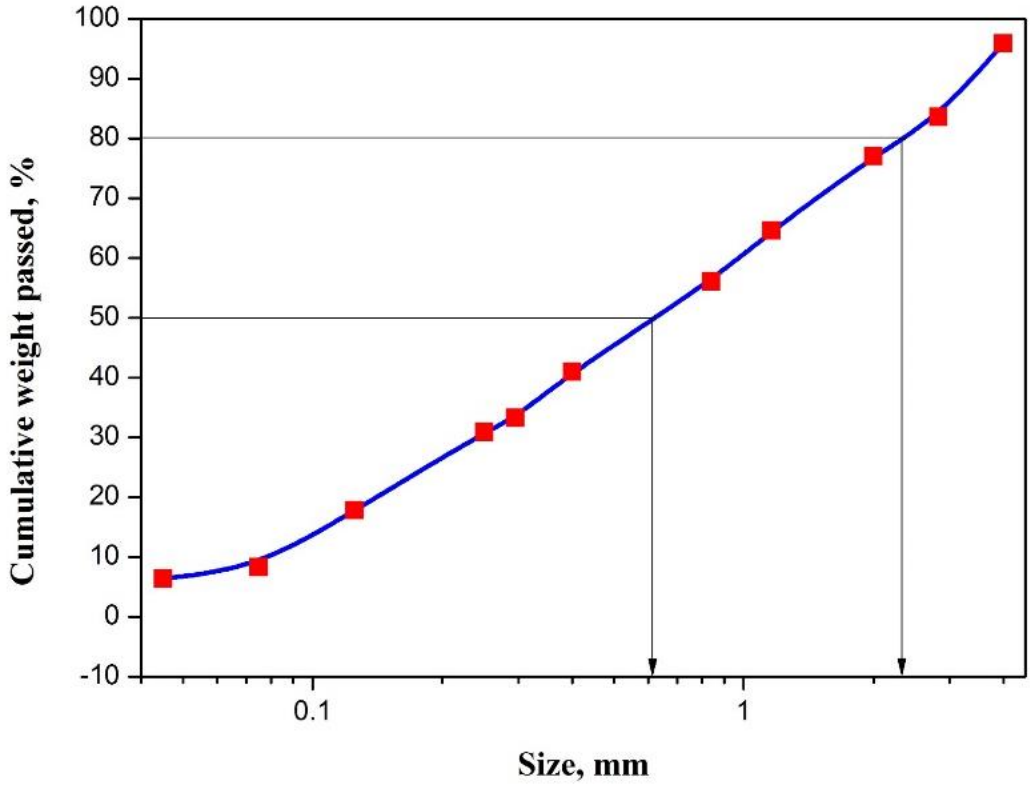

Fig. (6): Sieve analysis of crushed manganese size fractions.

Chemical analysis of the dry size distributions of crushed manganese sample is shown in Table (2). It is evident from the chemical analysis that the (+500µm) size fraction is rich in impurities. Also, (-500µm) size fractions are relatively rich in manganese compared with other fractions, and the sample appears to be more liberated in size fractions below 500µm as the content of MnO increases. While L.O.I (carbonates contained) is constant in all fractions, indicating that the carbonate impurities are finally disseminated in the crystal structure.

These results indicated that the sample may be beneficiated using magnetic separators such as Carpco, which were hardly removed in the ordinal conditions. The sample needs more grinding or dividing of less than 500um into fractions to show which fraction is more liberated than the other. In other words, to confirm and determine the best size fraction of manganese ore to concentrate, some size fractions were selected after crushing and grinding, such as (500+250µm) and (-250+75µm) using dry magnetic separators. From a technical point of view, dry magnetic separators will be effective for feed samples finer than 500µm and more than 75µm. So, the -75µm size fraction was excluded because of the slimes problems, which decreased the separation efficiency. The -5mm crushed sample was ground to -500µm by using a laboratory ball mill. The three fractions of the milled manganese sample and its chemical analysis are illustrated in Table (3).

Table (2): Chemical analysis of the size fractions of crushed manganese sample.

Size, mm	Wt.%	MgO%	Al_2O_3%	SiO_2%	CaO%	MnO%	L.O.I%
(+4)	4.1	11.6	2.7	7.4	20.2	21.4	32.2
(-4+2.83)	12.3	9.6	2.5	6.8	17.4	27.6	31.4
(-2.83+2)	6.6	10.4	2.4	6.6	18.3	26.5	31.5
(-2+1.16)	12.4	9.3	2.5	6.5	16.8	29.7	30.7
(-1.16+0.84)	8.5	8.4	2.1	6.1	15.7	33.4	29.8
(-0.84+0.4)	15.1	10.1	2.3	6.4	17.6	29.4	29.7
(-0.4+0.295)	7.7	9.8	2.1	5.9	17.3	30	30.6
(-0.295+0.250)	2.4	9.7	2	5.7	15.8	33.6	28.5
(-0.250+0.125)	13.1	8.8	1.9	5.4	16.6	32.1	31.3
(-0.125+0.075)	9.5	7.1	1.3	3.9	14.5	37.3	31.8
(-0.075+0.045)	1.9	8.6	1.3	3.9	17.8	33.1	32.6
-0.045	6.4	8.3	1.8	4.8	15.6	37.4	28.5
Feed%	100	8.28	2.1	5.8	15.56	30.58	29.5

Table (3): Complete chemical analysis of the three fractions of a milled sample.

Size, µm	Wt.%	MgO	Al_2O_3	SiO_2	K_2O	CaO	MnO	Fe_2O_3	L.O.I.
-500 +250	40.16	7.61	2.13	6.03	1.63	16.60	31.60	1.1	29.65
-250 +75	49.84	7.95	1.60	4.65	1.4	16.50	30.70	0.98	31.00
-75	10.0	13.66	1.28	10.36	0.84	12.58	29.45	0.86	23.15
Feed	100	8.28	2.10	5.80	1.02	15.56	30.58	1.03	29.5

4.3. Magnetic separation of the sample without attrition scrabbling

Table (4) illustrates the chemical analysis of Carpco dry magnetic separation at 1.5 Ampere for (-500 +250µm) and (-250 +75µm) size fractions. The grade of MnO increased from 31.6 to 41.66%, with a 28.34% recovery in -500+250 um size fraction. Also, in the -250+75um size fraction, the grade of MnO increased from 30.7 to 38.98%, with 31.23% recovery. The recovery of the concentrate (magnetic fraction) is low because the magnetic intensity is not enough to separate most manganese particles.

Table (4): Chemical analysis of Carpco dry magnetic separation at 1.5 Ampere.

Size, µm	Product	Wt.%	MgO	Al_2O_3	SiO_2	CaO	MnO	LOI	R.
-500 +250	Magnetic	21.5	7.35	1.99	4.92	12.21	41.66	26.14	28.34
	Non	78.5	7.68	2.19	6.34	17.59	29.25	30.86	
Feed		100	7.61	2.13	6.03	16.6	31.6	29.65	
-250 +75	Magnetic	27.8	8.87	1.32	3.69	13.51	38.98	26.91	31.23
	Non	72.2	7.6	1.74	5.1	17.75	28.11	30.36	
Feed		100	7.95	1.6	4.65	16.5	30.7	31	

Table (5) shows the chemical analysis of Carpco dry magnetic separation at 2.5 Ampere for (-500 +250µm) and (-250 +75µm) size fractions. The recovery of the concentrate (magnetic fraction) was increased to 47.52 and 56.94%, and the grade of MnO increased to 41.03 and 38.98%, for (-500 +250µm) and (-250 +75µm) size fractions, respectively, but the grade and recovery still low. Table (6) illustrates the chemical analysis of Carpco dry magnetic separation at 3.5 Ampere for (-500 +250µm) and (-250 +75µm) size fractions. The grade of MnO increased from 31.6 to 35.50%, with 71.89% recovery in -

500+250um size fraction. Also, in the -250+75um size fraction, the grade of MnO increased from 30.7 to 30.84%, with a 64.49% recovery. Figure (7) shows the results of magnetic separation at different magnetic intensities. By increasing magnetic intensity, the MnO content decreased slightly while manganese recovery increased significantly. These results are because the non-magnet impurities cover the manganese particle surfaces. So, the attrition scrubbing process is required to clean the manganese particle surfaces.

Table (5): Chemical analysis of Carpco dry magnetic separation at 2.5 Ampere.

Size, µm	Product	Wt.%	MgO	Al_2O_3	SiO_2	CaO	MnO	LOI	R.
(-500 +250)	Magnetic	36.6	7.41	2.1	4.94	11.42	41.03	26.38	47.52
	Non	63.4	7.93	2.29	6.79	19.5	25.94	31.84	
Feed		100	7.61	2.13	6.03	16.6	31.6	29.65	
(-250 +75)	Magnetic	53	7.35	1.55	4.15	13.89	33.95	29.37	56.94
	Non	47	8.87	1.72	5.4	19.22	26.86	33.63	
Feed		100	7.95	1.6	4.65	16.5	30.7	31	

Table (6): Chemical analysis of Carpco dry magnetic separation at 3.5 Ampere.

Size, µm	Product	Wt.%	MgO	Al_2O_3	SiO_2	CaO	MnO	L.O. I	R.
(-500 +250)	Magnetic	64	7.03	2.15	5.43	15.52	35.5	28.07	71.89
	Non	36	8.94	2.25	7.32	19.05	25.45	32.96	
Feed		100	7.61	2.13	6.03	16.6	31.6	29.65	
(-250 +75)	Magnetic	64.2	7.48	1.61	4.44	15.07	30.84	30.73	64.49
	Non	35.8	9.42	1.72	5.53	19.32	29.32	33.68	
Feed		100	7.95	1.6	4.65	16.5	30.7	31	

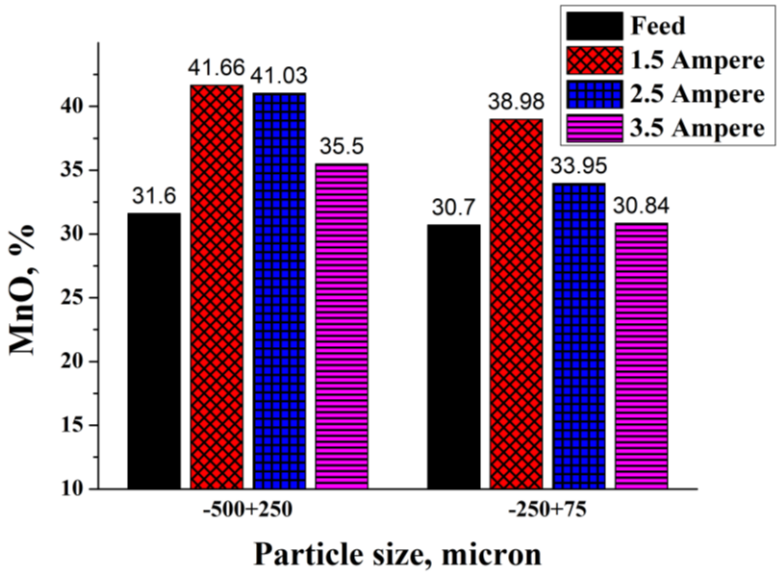

Figure (7): Results of magnetic separation at different magnetic intensities.

4.4. Effect of attrition scrubbing process on manganese content

Table (7) illustrates the chemical analysis of the three fractions after the attrition scrubbing process at 30 min. attrition time, 1800rpm attrition speed and 65% pulp density. The attrition scrubbing process leads to an increase in MnO content from 31.6 to 33.72% in the (-500 +250µm) size fraction and from 30.7 to 32.19% in the (-250 +75µm) size fraction. This is because non-magnetic impurities are removed from the manganese particle surface.

Table (7): The results after attrition scrubbing.

Size, µm	Wt.%	MgO	Al_2O_3	SiO_2	K_2O	CaO	MnO	Fe_2O_3	L.O.I.
-500+250	30.15	8.82	2.71	6.66	1.23	16.96	33.72	1.02	30.81
-250+75	59.62	8.93	1.96	4.32	1.37	15.88	32.19	1	27.82
-75	10.23	14.66	1.68	11.5	0.84	12.62	17.22	1.37	38.15
Feed	100	8.28	2.1	5.8	1.02	15.56	30.58	1.03	29.5

4.5. Effect of attrition scrubbing process on improving magnetic separation

Table (8) shows the chemical analysis of Carpco dry magnetic separation after attrition scrubbing at 2.5 Ampere for (-500 +250µm) and (-250 +75µm) size fractions. MnO content increased from 33.72 to 40.12%, with a 77.22% recovery in the case of -500+250um size fraction. Also, in the case of size -250+75um size fraction, the MnO content increased from 35.19 to 44.28%, with 84.93% recovery. Table (9) illustrates the chemical analysis of Carpco dry magnetic separation at 3.5 Ampere for (-500 +250µm) and (-250 +75µm) size fractions. The grade of MnO increased from 33.72 to 44.12%, with 85.66% recovery in the case of -500+250um size fraction. Also, in the case of size -250+75um size fraction, the grade of MnO increased from 35.19 to 40.23%, with 75.45% recovery. Figure (8) shows the results of magnetic separation after the attrition scrubbing process at different magnetic intensities. These results were because the attrition scrubbing process liberated the manganese particle surfaces from non-magnet impurities which covered the manganese particle surfaces.

Table (8): Chemical analysis of Carpco dry magnetic separation after attrition scrubbing at 2.5 Ampere.

Size, µm	Product	Wt.%	MgO	Al_2O_3	SiO_2	CaO	MnO	Fe_2O_3	LOI	R.
(-500 +250)	Magnetic	64.9	6.55	1.76	4.6	12.93	40.12	0.75	25.26	77.22
	Non	35.1	8.04	2.86	7.24	19.58	20.97	0.86	34.28	
Feed%		100	6.82	2.13	6	15.6	33.72	0.79	28.01	
(-250 +75)	Magnetic	67.5	6.66	1.38	2.37	12.54	44.28	0.81	26.11	84.93
	Non	32.5	9.68	1.45	4.34	18.87	15.86	0.76	41.38	
Feed%		100	7.64	1.5	3.44	14.44	35.19	0.77	24.11	

Table (9): Chemical analysis of Carpco dry magnetic separation after attrition scrubbing at 3.5 Ampere.

Size, µm	Product	Wt.%	MgO	Al_2O_3	SiO_2	CaO	MnO	LOI	R.
(-500 +250)	Magnetic	65.47	6.11	1.94	4.76	13.33	44.12	24.26	85.66
	Non	34.53	8.64	2.72	8.69	20.93	15.14	34.58	
Feed		100	6.82	2.13	6	15.6	33.72	28.01	
(-250 +75)	Magnetic	66	6.99	1.12	2.28	13.11	40.23	23.08	75.45
	Non	34	8.24	1.56	4.8	16.14	25.46	26.83	
Feed%		100	7.42	1.5	3.44	14.44	35.19	24.11	

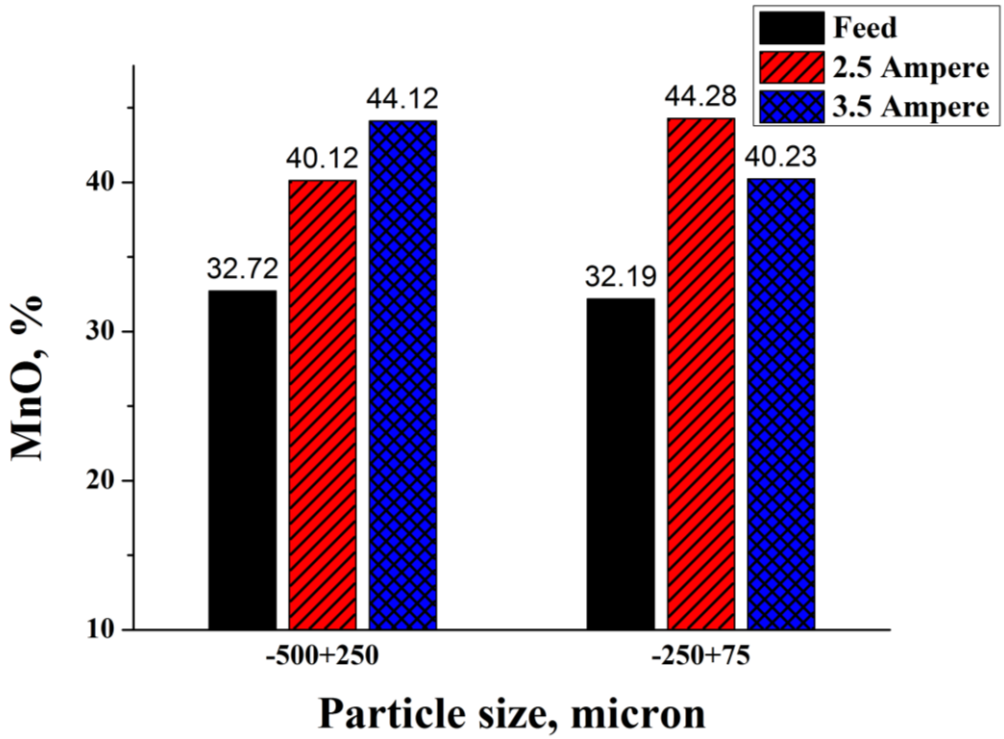

Figure (8): Results of magnetic separation after attrition scrubbing process.

5. CONCLUSIONS

The mineralogical study showed that the ore mainly contains pyrolusite and different types of minerals such as dolomite, calcite, quartz, and gypsum. So, it is expected that upgrading the ore using the magnetic separation technique is possible because pyrolusite has a significant difference in its magnetic susceptibility. Using Carpco dry magnetic separation at 2.5 Ampere without attrition scrubbing produced a concentrate with suitable grade (41.03% MnO) but with low recovery (47.52%) in (-500 +250um) size fraction. Also, the results revealed that at 2.5 Ampere, a concentrate containing 38.98% MnO with 26.91% recovery is obtained in the size fraction of (-250 +75µm). This result is because the non-magnet impurities cover the manganese particle surfaces. A combination of

aggressive attrition scrubbing and Carpco dry magnetic separation at 3.5 Ampere succeeded in increasing the MnO content from 31.60% in (-500 +250um) size fraction of the original sample to 44.12% in the concentrated sample, with recovery 77.22%. Meanwhile, MnO content increased from 30.70 % in the (-250+75um) size fraction of the original sample to 44.28 % in the concentrated sample at 2.5 Ampere, with a recovery of 84.93%. These results were because the attrition scrubbing process cleaned the manganese particle surfaces. Due to the low energy consumption and the current environmental protection requirements, magnetic separation without calcination was selected in this study

6. REFERENCES

1. Luo, Z., Shu, J., Chen, M., Wang, R., Zeng, X., Yang, Y., ... & Deng, Y. (2021). Enhanced leaching of manganese from low-grade pyrolusite using ball milling and electric field. *Ecotoxicology and Environmental Safety*, *211*, 111893.
2. Srivani, P., & Noothana, P. (2019). Beneficiation of manganese ore using froth flotation technique. *Materials Today: Proceedings*, *18*, 2279-2287.
3. Xiong, S., Li, X., Liu, P., Hao, S., Hao, F., Yin, Z., & Liu, J. (2018). Recovery of manganese from low-grade pyrolusite ore by reductively acid leaching process using lignin as a low cost reductant. *Minerals Engineering*, *125*, 126-132.
4. Singh, V., Ghosh, T. K., Ramamurthy, Y., & Tathavadkar, V. (2011). Beneficiation and agglomeration process to utilize low-grade ferruginous manganese ore fines. *International Journal of Mineral Processing*, *99*(1-4), 84-86.
5. Xin, Z., Wang, M. L., Burow, G., & Burke, J. (2009). An induced sorghum mutant population suitable for bioenergy research. *BioEnergy Research*, *2*, 10-16.
6. Zhang, X., Tan, X., Yi, Y., Liu, W., & Li, C. (2017). Recovery of manganese ore tailings by high-gradient magnetic separation and hydrometallurgical method. *Jom*, *69*, 2352-2357.
7. Lei, M., Ma, B., Lv, D., Wang, C., Asselin, E., & Chen, Y. (2021). A process for beneficiation of low-grade manganese ore and synchronous preparation of calcium sulfate whiskers during hydrochloric acid regeneration. *Hydrometallurgy*, *199*, 105533.
8. Chen, G., Jiang, C., Liu, R., Xie, Z., Liu, Z., Cen, S., ... & Guo, S. (2021). Leaching kinetics of manganese from pyrolusite using pyrite as a reductant under microwave heating. *Separation and Purification Technology*, *277*, 119472.
9. Baba, A. A., Ibrahim, L., Adekola, F. A., Bale, R. B., Ghosh, M. K., Sheik, A. R., ... & Folorunsho, I. O. (2014). Hydrometallurgical processing of manganese ores: a review. *Journal of minerals and materials characterization and engineering*, *2*(3), 230-247.
10. Wu, F. F., Zhong, H., Wang, S., & Lai, S. F. (2014). Kinetics of reductive leaching of manganese oxide ore using cellulose as reductant. *Journal of Central South University*, *21*, 1763-1770.
11. Chen, J., Li, L., Chen, G., Peng, J., & Srinivasakannan, C. (2017). Rapid thermal decomposition of manganese ore using microwave heating. *Journal of Alloys and Compounds*, *699*, 430-435.

12. Li, K., Chen, J., Peng, J., Omran, M., & Chen, G. (2020). Efficient improvement for dissociation behavior and thermal decomposition of manganese ore by microwave calcination. Journal of cleaner production, 260, 121074.
13. Gao, Y., Olivas-Martinez, M., Sohn, H. Y., Kim, H. G., & Kim, C. W. (2012). Upgrading of low-grade manganese ore by selective reduction of iron oxide and magnetic separation. *Metallurgical and Materials Transactions B*, *43*, 1465-1475.
14. Andrade, E. M., Costa, B. L. C. M., Alcântara, G. A. G., & Lima, R. M. F. (2012). Flotation of manganese minerals and quartz by sodium oleate and water glass. *Latin American applied research*, *42*(1), 39-43.
15. Pereira, M. J., Lima, M. M. F., & Lima, R. M. F. (2014). Calcination and characterization studies of a Brazilian manganese ore tailing. *International Journal of Mineral Processing*, *131*, 26-30.
16. Sun, D., Li, M. L., Li, C. H., Cui, R., & Zheng, X. Y. (2014). A green enriching process of Mn from low grade ore of manganese carbonate. *Applied Mechanics and Materials*, *644*, 5427-5430.
17. Akbar, M. R., & Mohammad, R. H. (2013). Characterization and Beneficiation of Iranian Low-Grade Manganese Ore. *Physicochemical Problems of Mineral Process in Journal*, *50*, 982-993.
18. MALAYOĞLU, U. (2010). Study on the gravity processing of manganese ores. *Asian Journal of Chemistry*, *22*(4).
19. Lin, S., Li, K., Yang, Y., Gao, L., Omran, M., Guo, S., ... & Chen, G. (2021). Microwave-assisted method investigation for the selective and enhanced leaching of manganese from low-grade pyrolusite using pyrite as the reducing agent. *Chemical Engineering and Processing-Process Intensification*, *159*, 108209.
20. Zhang, Y., You, Z., Li, G., & Jiang, T. (2013). Manganese extraction by sulfur-based reduction roasting–acid leaching from low-grade manganese oxide ores. *Hydrometallurgy*, *133*, 126-132.
21. Yuan, S., Zhou, W., Han, Y., & Li, Y. (2020). Separation of manganese and iron for low-grade ferromanganese ore via fluidization magnetization roasting and magnetic separation technology. *Minerals Engineering*, *152*, 106359.
22. Gao, L., Liu, Z., Pan, Y., Feng, C., Ge, Y., & Chu, M. (2020). A study on separation of Mn and Fe from high-alumina ferruginous manganese ores by the carbothermal roasting reduction process. *Advanced Powder Technology*, *31*(1), 51-60.
23. Rehman, W. U., Rehman, A. U., Khan, F., Muhammad, A., & Younas, M. (2020). Studies on beneficiation of manganese ore through high intensity magnetic separator. *Advances in Sciences and Engineering*, *12*(1), 21-27.